International Journal of Chemical, Materials and Biomolecular Sciences
ISSN: 2415-6620
Vol:11, No:2, 2017

Influence of Sodium Acetate on Electroless Ni-P Deposits and Effect of Heat Treatment on Corrosion Behavior

Y. El Kaissi, M. Allam, A. Koulou, M. Galai, M. Ebn Touhami

Abstract**—**The aim of our work is to develop an industrial bath of nickel alloy deposit on mild steel. The optimization of the operating parameters made it possible to obtain a stable Ni-P alloy deposition formulation. To understand the reaction mechanism of the deposition process, a kinetic study was performed by cyclic voltammetry and by electrochemical impedance spectroscopy (EIS). The coatings obtained have a very high corrosion resistance in a very aggressive acid medium which increases with the heat treatment.

Keywords**—**Ni–P coating, electrochemical impedance spectroscopy, heat treatment, cyclic voltammetry, potentiodynamic polarization.

I. Introduction

ELECTROLESS nickel (EN) coating offer a wide range of possibilities of manufacture with important economic benefits, technological and environmental, this justifies the orientation of the researchers to improve the quality of the coating's baths of these alloys [1], [2]. Today, the Ni–P alloys are widely used in various industrial applications such as chemical engineering, mechanical and industrial engineering, automobile engineering, electronics and aerospace industry etc.

The Ni–P deposits show a as high corrosion resistance, high wear resistance, low friction coefficient, good lubricity, high hardness [2], [3]. It is generally accepted that the coating rate, structure and properties of Ni–P alloys mainly depend upon the constituents' concentrations of the plating bath, type of the reducing agent, complexing agent, stabilizer, pH and bath temperature [4], [5]. The Heat-treatment plays also an important role in improving the performance of electroless-plated Ni–P by affecting the thickness, structure and morphology of deposit. During thermal processing, the amorphous and microcrystalline structure transforms into a crystalline structure containing mainly Ni and its phosphides. However, with higher thermal treatment temperatures, the Ni–P becomes the dominant phosphide phase as like as it is more stable. The transformation into crystalline structure is mainly observed when the EN coating is heated at temperatures above 300°C. In some investigations, the intermediate phases of Ni_5P_2 and $Ni_{12}P$ have been detected [6]-[8]. The aim of this work is to study the influences of additive (sodium acetate) and heat treatment on deposition rate, surface morphology, microstructure of Ni–P coating and its corrosion characteristics in 4M H_3PO_4 solution. The voltammetric studies and EIS of the effect of additive (sodium acetate) were also evaluated and discussed.

Y. El Kaissi is with the Laboratory of Material Engineering and Environment: Modeling and Application, Ibn Tofail University, Faculty of Sciences Kenitra, Morocco (Corresponding author; e-mail: yassine.elkaissi@gmail.com).

II. Experimental Procedures

The EN bath formulation and operating conditions were illustrated by Table I contained nickel sulfate as a metal ion source, sodium hypophosphite as a reducing agent, sodium citrate as a complexing agent, and sodium acetate as an additive. The pH was maintained at 5.50 ± 0.01 with by adding acetic acid, which plays a buffer role and the temperature was held at 85 ± 2°C.

The substrates were a mild steel plate of dimensions (L = 2 cm, l = 1 cm and h = 0.2 cm), polished using abrasive paper up to 1200 grade, cleaned with acetone, etched in 10% dilute sulphuric acid, rinsed with distilled water, and dried.

The Ni-P samples were annealed at 200, 400, 600 and 800 °C for a duration of 1 hour in heating furnace. After thermal treatment, the samples are cooled under ambient conditions.

The surface morphology of the as-deposited Ni-P was investigated by using the scanning electron microscopy (SEM) connected with EDX unit and the crystalline structure was studied by the X-ray diffractometer (XRD).

The Electrochemical measures were performed by using a potentiostat (VoltaLab model PGZ100) monitored by a personal computer. The reference electrode was a saturated calomel electrode (SCE) with all potentials referred.

TABLE I
Baths Compositions and Operating Conditions of Ni-P Electroless Deposition

Bath composition and operating conditions	Values
Nickel sulfate	30 $g.L^{-1}$
Sodium hypophosphite	23 $g.L^{-1}$
Sodium citrate	10 $g.L^{-1}$
Sodium acetate	0-30 $g.L^{-1}$
Temperature	85 ± 2 °C
pH	5,5 ± 0,01

III. Results And Discussion

A. Deposition Rate

The addition of sodium acetate to the bath of basis causes a net improvement in the speed of the process of electroless, and the evolution of the deposition rate as a function of the

concentration of sodium acetate (Fig. 1). In this case, the speed of the bath of chemical deposit of the alloy Ni-P reaches 12.7 µm.h^{-1} for a concentration of sodium acetate of 20 g.L^{-1}. Such a concentration of this additive is used to increase the speed of chemical deposit of the alloy Ni-P of more than 340% compared to the bath of basis. This can be explained by the mechanism of action of accelerators by the elimination of H^+ ions which occupy the active sites of the substrate and activate as well the process of electroless [9]. These H^+ ions produce by the oxidation of hypophosphite on the substrate according to (1), (2):

$$H_2PO_2^- + H_2O \rightarrow H_2PO_3^- + 2H^+ + 2e^- \quad (1)$$

$$H_2PO_2^- + 2H_2O \rightarrow H_2PO_4^- + 4H^+ + 4e^- \quad (2)$$

This elimination of H+ ions is demonstrated by the release of hydrogen at the level of the substrate according to the overall electroless reaction (3), or by recombination of H^+ ions according to the reactions:

$$Ni^{2+} + H_2PO_2^- + 2H_2O \rightarrow Ni + H_2PO_3^- + 2H^+ + H_2 \quad (3)$$

$$H^+ + e^- \rightarrow H \quad (4)$$

$$H + H \rightarrow H_2 \quad (5)$$

For concentrations greater than 20 g.L^{-1} of the additive in the bath of basis there is a decrease in the deposition rate, this may be due to the sodium acetate, which is adsorbed on the surface and blocks the active sites resulting in a lowering of the rate of load transfer or nucleation. Beyond a concentration of 30 g.L^{-1} of the additive, we are witnessing a spontaneous decomposition of the electroless bath as soon as the first minutes.

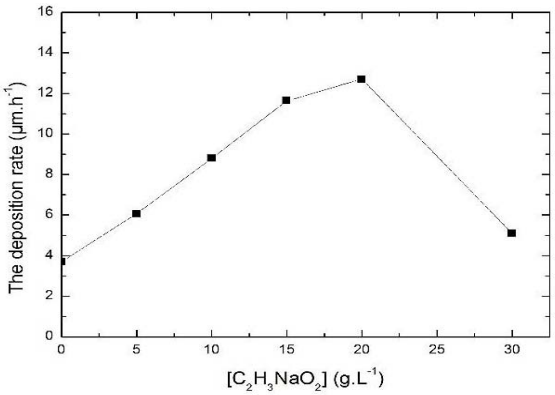

Fig. 1 Effect of sodium acetate concentration on deposition rate of Ni-P electroless deposition

B. Kinetics Studies

1. Cyclic Voltammetry Studies

In order to determine the kinetic processes involved in the autocatalytic chemical deposition of nickel, an electrochemical study by cyclic voltammetry of the bath in the presence of the additive is carried out using platinum as the working electrode.

Fig. 2 shows the voltammogram recorded under the following conditions:

- The scanning potential ranges from 1000 mV (starting potential) to -1000 mV (inversion potential).
- The scanning speed is set to 10 mV.s^{-1}.

The recorded voltammogram shows the general pattern of chemical deposition of the Ni-P alloy. This diagram is characterized by:

- A cathodic peak K related to the reduction of Ni^{2+}, $H_2PO_2^-$ and H^+ ions [10].
- Three anodic peaks in the oxidation of certain compounds or in the dissolution of deposited species. Peak A appears towards -800 mV / SCE relative to the oxidation of the anion hypophosphite [11], [12], whereas the two peaks B and C are related to the dissolution of the Ni-P alloy in two steps :
  - The first dissolution appears towards -300 mV/SCE (peak B), corresponding to the dissolution of the crystalline phase of the phosphorus-poor Ni-P alloy [13].
  - At positive potentials, the oxidation of the amorphous phase of the Ni-P alloy rich in phosphorus (peak C) is observed.

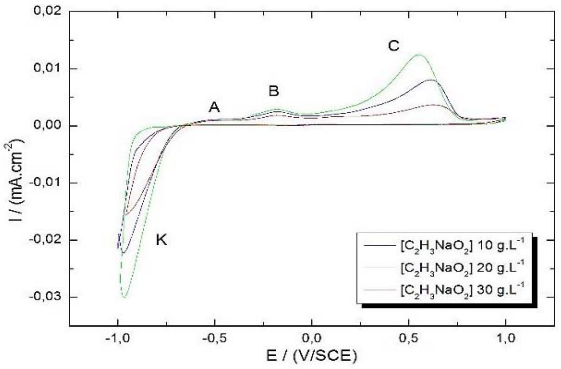

Fig. 2 Cyclic voltammogram recorded on Pt electrode from the Ni-P electroless bath (Table I) at scan rate of 10 mV.s^{-1}

From these results, it can be argued that the intensities of the anodic and cathodic peaks of the chemical deposition reaction are correlatively related to the concentration of sodium acetate. This means that increasing the concentration of sodium acetate promotes the oxidation of hypophosphite and therefore the reduction of nickel. These results are in agreement with the results of the deposition rate calculated by the gravimetric method.

2. EIS Studies

The deposition potential is characterized by a current equal to 0, resulting from two simultaneous anodic and cathodic processes. Fig. 3 shows the impedance diagram recorded at different concentrations of sodium acetate.

On the one hand, it is observed that this additive does not affect the general shape of the impedance diagram. The impedance diagram shows the existence of a high frequency

capacitive loop attributed to the relaxation of the double layer in parallel with the charge transfer resistor Rct. Its size decreases with increasing concentration of sodium acetate.

On the other hand, we find that increasing the concentration of compound A in solution increases the charge transfer resistance (Rt), indicating that there is a phenomenon of inhibition of the deposition process by the sodium acetate, confirming the results obtained by the gravimetric measurements.

It should be noted that the double layer capacitance (Cct) value was affected by surface imperfections, and this effect was simulated by a constant phase element (CPE) [14].

The use of Qct and n parameter is justified in the case that their changes are related to the heterogeneity of surface resulting from the surface roughness. The impedance of the CPE is stated as:

$$Z = \frac{R}{1+R\times \mathrm{CPE}(j\omega)^{\alpha}} \quad (6)$$

The corresponding simulated impedance parameters are listed in Table II.

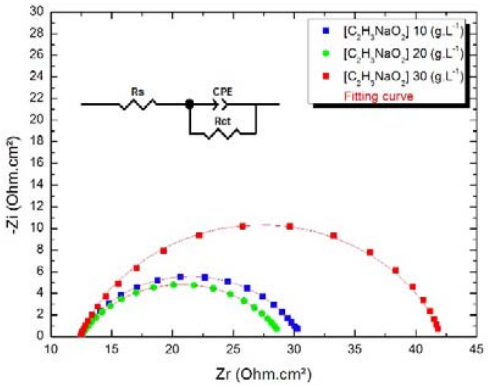

Fig. 3 Electrochemical impedance spectra obtained at deposition potential containing different concentrations of sodium acetate concentrations. Equivalent circuit models used to fit the experiment impedance data

TABLE II
ELECTROCHEMICAL PARAMETERS FOR ELECTROLESS NI-P DEPOSITS IN THE PRESENCE OF DIFFERENT CONCENTRATIONS OF SODIUM ACETATE

[$NaCH_3COO$] g.L^{-1}	R_e Ohm.cm^2	Q_{ct} mF.$s^{(n-1)}$	n_{ct}	R_{ct} Ohm.cm^2
10	12,38	2,498	0,7003	18,19
20	12,42	4,257	0,6679	16,6
30	12,4	1,554	0,7728	29,8

C. Surface Morphology and Microstructure of Deposits

Fig. 4 presents the results of SEM of the surfaces of Ni-P alloys deposited in the absence and in the presence of sodium acetate. These micrographs show that the deposits are characterized by a nodular aspect as well as the addition of sodium acetate to the electroless bath has a significant influence on the general morphology of the deposits Ni-P, the sodium acetate addition promotes the increase in the number and diameter of the individual nodules in deposits Ni-P.

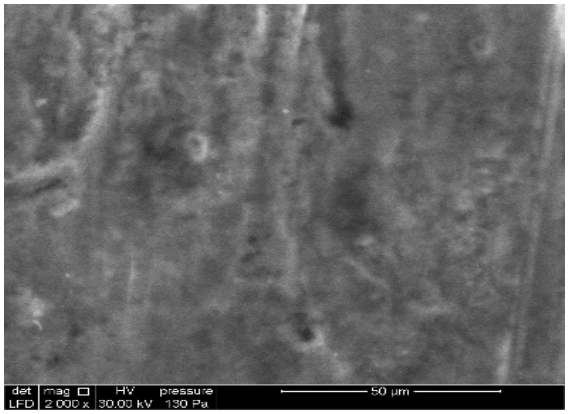

(a)

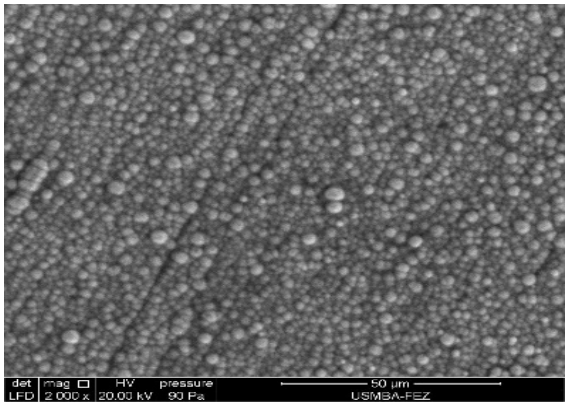

(b)

Fig. 4 SEM surface morphology of Ni-P coatings in (a) the absence and (b) the presence of 20g.L^{-1} of sodium acetate

Fig. 5 shows the diffraction patterns in the alloy Ni-P deposits as-coated and heat treated for one hour at different temperatures (i.e. 200°C, 400°C, 600°C and 800°C). Only a broad peak can be distinguished in the diffraction pattern of X-rays of the deposit Ni-P coated, indicating an amorphous structure [15]. There were no significant changes in the diffraction pattern of the X-ray Ni-P deposit treated at 200°C, indicating that no phase transition occurring in this temperature range. When the heat treatment temperature was increased to 400 °C, the structure became crystalline and new peaks corresponding to Ni and Ni_3P appeared. This behavior can be attributed to pure nickel crystallization followed by nickel phosphide precipitation Ni3P solid solution nickel-phosphorous that is supersaturated [16]-[18]. The beginning of the allotropic transformation of the Ni-P alloy occurred between 400 and 600 °C. The study similar systems [19], [20] concluded that crystalline Ni-P alloys are denser than those of microcrystalline and amorphous of the same chemical composition and the transition of the crystalline structure in the amorphous accompanied by a contraction of volume [17]. In the X-ray diffraction profile of Ni-P alloy treated at 800°C, the presence of crystalline diffraction lines mainly coming from nickel and Ni5P2 was observed [21]-[23], the presence

of phosphorus may be the reason for the creation nickel phosphides, and activating the electroless Ni-P deposition at elevated temperature.

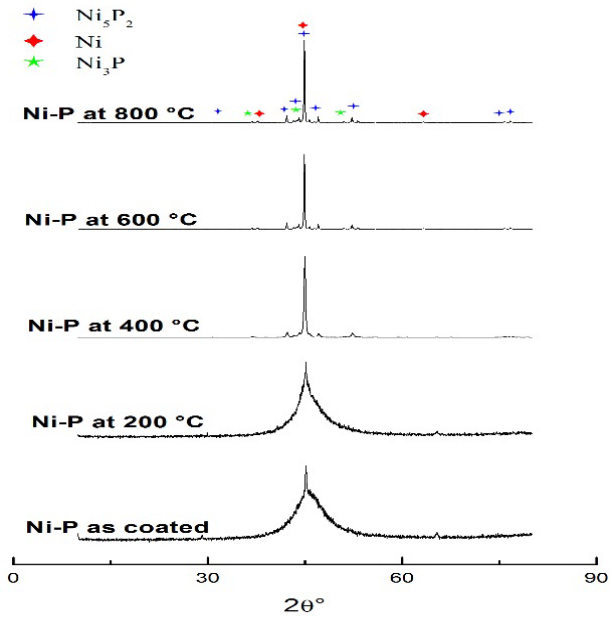

Fig. 5 XRD spectra of electroless Ni–P coatings measured before and after heat treated at different conditions

D.Corrosion Study

1. Potentiodynamic Polarization Studies

The corrosion behavior of the mild steel and the Ni-P alloys as-deposited and after thermal treatment at different temperatures was measured at room temperature with polarization curves measurement in 4M H3PO4. The electrochemical kinetic parameters (corrosion potential (Ecorr), corrosion current density (Icorr) and Tafel cathode slope (βc), determined from these experiments by extrapolation method [24] are presented in Table III. Icorr was determined by extrapolating Tafel only from the cathodic polarization curve alone, which usually produces a longer and better defined Tafel region [25].

Fig. 6 shows the corrosion behavior of steel substrate, Ni-P alloys as-deposited and treated at different temperatures in an acid medium. The shape of the overall polarization curve obtained in 4M H3PO4 medium is similar to those found by some authors for electroless plating of Ni-P in HCl and H2SO4 mediums [26]-[29]. It is observed that in the anode branch, the current density decreases significantly in the presence of Ni-P coating, indicating the good resistance of this coating. The results also show a tendency for passivation in 4M phosphoric acid by the appearance of a common plate in anodic polarization. The existence of this current plateau has been reported on these types of alloys [26], [29].

The corrosion current density of the Ni-P coatings clearly decreased with the annealing temperature to 400°C and increased when the temperature increased to 800°C (Table III). The lower corrosion current density implied a lower dissolution rate and better corrosion resistance. The rate of dissolution apparently depended on the amount of the uniform composition, the crystalline interfaces, the electrochemical stability and the compactness of the passive film. It is well known that the phosphorus content is strongly related to the crystalline state. The formation of a phosphorus-rich surface layer at the alloy/solution interface is a consequence of the rapid and selective dissolution of nickel. This process of dissolution is controlled by the diffusion of nickel in this area rich in phosphorus [30], [31]. According to other publications, the dissolution of the surface preferably enriched in external phosphorus reacts with water to form a layer of hypophosphite $H_2PO_2^-$ anions [27], [29], [32]. This layer in turn makes it possible to block the water supply to the surface of the electrode, which prevents the hydration of the nickel [33], [34] which is considered the first step to form soluble Ni^{2+} species.

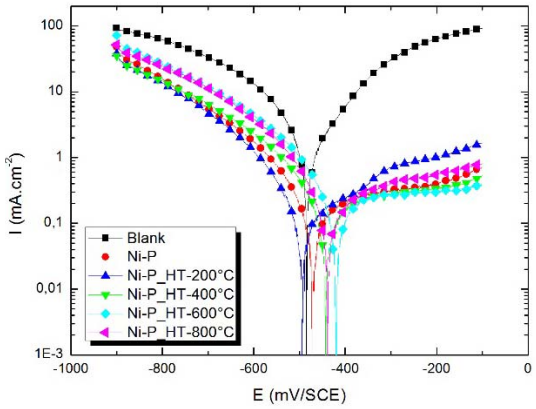

Fig. 6 Polarizations curves of the mild steel, the electroless Ni–P coatings as-plated and heat treated at different temperatures in 4M H_3PO_4: experimental and fitted data

Therefore, after the thermal treatments process, the Ni-P deposits underwent volume contraction due to the release of gaseous hydrogen. The heated Ni-P coatings at higher temperatures than 400°C are broken and easy to dissolve, which leads to a higher corrosion current density than the deposited coatings. The annealed coating at 400°C had a lower corrosion current density than the annealed coating at 200°C due to the significant recrystallization of Ni, P and Ni3P at 400°C resulting in a decrease in the crystal interfaces.

TABLE III
POLARIZATION PARAMETERS OF THE MILD STEEL, THE ELECTROLESS NI–P COATINGS AS-PLATED AND HEAT TREATED AT DIFFERENT TEMPERATURES IN 4M H_3PO_4

	$-E_{corr}$ vs. SCE mV	**I_{corr}** $\mu A.cm^{-2}$	**-βc** $mV.dec^{-1}$
Blank	485, 5	4832, 7	248, 7
Ni-P	472,3	413, 2	190,7
Ni-P_HT-200°C	495	327,3	173,1
Ni-P_HT-400°C	441, 1	258,2	160
Ni-P_HT-600°C	421,4	506,5	193
Ni-P_HT-800°C	439,6	544,5	199, 8

2. EIS Studies

Fig. 8 shows the Nyquist plots obtained for mild steel substrate, Ni-P alloy and heat-treated at different temperatures in 4M H3PO4 solution at their open circuit potential.

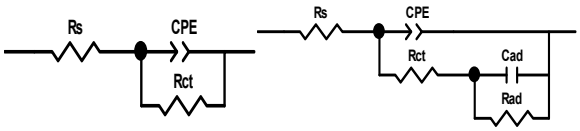

(a) (b)

Fig. 7 Equivalent circuit models for (a) the mild steel, (b) the electroless Ni–P coatings as-plated and heat treated at different temperatures in 4M H_3PO_4

In the case of mild steel, the plots consist of a semi-circle that can be devoted to the response of a combination of transfer resistance (Rct) and constant phase element (CPE). In the presence of Ni-P alloys as-coated and annealed, all curves appear to be similar (Nyquist plots), composed of two semi-circles poorly separated of: The first which is located between the high frequency is the response of the charge transfer resistor (Rct), this resistance increases in the presence of Ni-P as coated and heat treated, but the second can be attributed to the adsorbed film, as it has been reported by other authors [28]. They attributed the second loop to the ability of an adsorbed film that is due to the formation of the oxide layer. To account for the corrosion of mild steel substrate and Ni-P coatings in the acidic environment in the discontinuity of potential, a model of the equivalent circuit given in Fig. 7 is used to simulate the metal/solution interface and analyze the Nyquist diagrams. It basically consists of the following: the electrolyte solution resistance (Rs), constant phase element (CPE), charge transfer resistance from the electrode / solution interface (Rct), adsorption capacity (Cad) and adsorption resistance (Rad).

TABLE IV
IMPEDANCE PARAMETERS FOR THE MILD STEEL, THE ELECTROLESS NI–P COATINGS AS-PLATED AND HEAT TREATED AT DIFFERENT TEMPERATURES IN 4M H3PO4

	R_e Ohm.cm^2	Q_{ct} µF.s$^{(n-1)}$	n_{ct}	R_{ct} Ohm.cm^2	C_{ad} µF.cm^{-2}	R_{ad} Ohm.cm^2
Blank	2,758	485,4	0,885	6,205		
Ni-P	2,912	104,1	0,843	424,9	435,3	39,9
Ni-P_HT 200°C	2,931	81,14	0,846	491,5	275,7	107,3
Ni-P_HT 400°C	2,964	58,21	0,808	525,7	38,2	144,5
Ni-P_HT 600°C	2,895	109	0,839	308,4	743,6	21,63
Ni-P_HT 800°C	2,817	122,2	0,822	305,5	767,7	16,95

Fig. 9 gives the comparison between the circuit model (Fig. 7) and experiment presented in Bode format, it is clear that the proposed models are representative of phenomena that can occur in the system studied in both the HF part in the LF part of the spectra.

From Table IV, It is noted that all the corrosion parameters of the annealed Ni-P coatings varied with the same trend, the charge transfer resistance (Rct) increased and CPE decreased, which means that the structures of Ni-P deposits have changed and become more dense and uniform after the heat treatment.

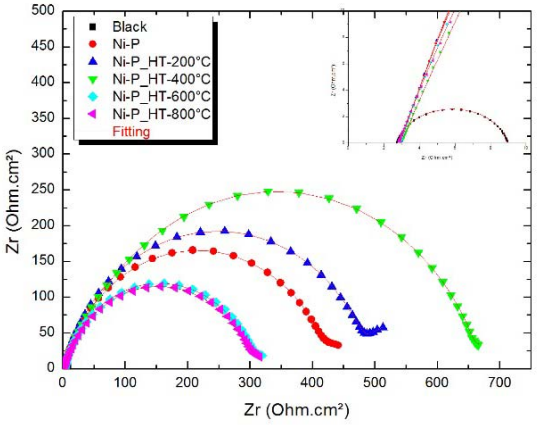

Fig. 8 EIS Nyquist diagrams for the mild steel, the electroless Ni–P coatings as-plated and heat treated at different temperatures in 4M H_3PO_4: experimental and fitted data

The high values of the charge transfer resistance (R_{ct}) obtained for the heat-treated Ni-P alloys of the present study imply a better corrosion protective capacity than the Ni-P as-coated.

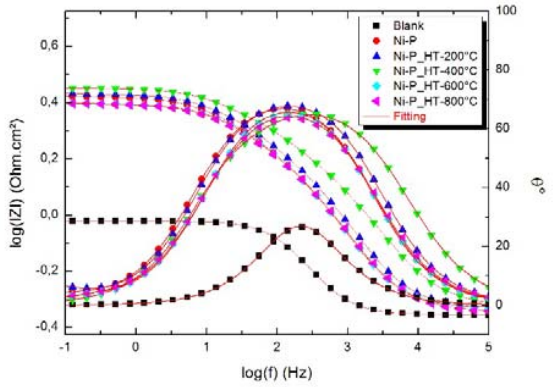

Fig. 9 EIS Bode diagrams for the mild steel, the electroless Ni–P coatings as-plated and heat treated at different temperatures in 4M H_3PO_4: experimental and fitted data

IV. Conclusions

In this present work, we have investigated the influence of sodium acetate as an additive on the formation and characteristics of electroless Ni–P deposits obtained using hypophosphite as a reducing agent.

- The deposit composition and the deposition rate depend strongly on the sodium acetate concentration.
- The electrochemical investigations confirm the effect of sodium acetate such as accelerator.

- X-ray diffraction studies revealed that a broad diffraction band corresponding to the amorphous nickel disappeared as a result of the transformation of the Ni-P system, and the occurrence of a diphase system in the heated coating was observed. This diphase system consisted of nickel crystallites and nickel phosphide crystallites of the type Ni_3P and Ni_5P_2.
- The corrosion resistance of Ni-P on mild steel is greatly improved by the heat-treatment which was tested by the potentiodynamic polarization experiment and by EIS in 4M H_3PO_4 medium.

REFERENCES

[1] C. Gu, J. Lian, G. Li, L. Niu, and Z. Jiang, Electroless Ni-P plating on AZ91D Magnesium alloy from a sulfate solution, J. of alloys and compounds vol. 39, 2005, pp. 104–109.
[2] C. J. Lin and J. L. He, Cavitations erosion behavior of electroless nickel-plating on AISI1045 Steel, Wear, vol. 259, 2005, pp. 154-159.
[3] YJ. Hu, L. Xiong and JL. Meng, Electron microscopic study on interfacial characterization of electroless Ni–W–P plating on aluminium alloy, Appl Surf Sci, vol. 253, 2007, pp. 5029–5034.
[4] D Dong, XH. Chen, WT. Xiao, GB .Yang and PY. Zhang, Preparation and properties of electroless Ni–P–SiO2 composite coatings. Appl Surf Sci, vol. 255, 2009, pp 7051–7055.
[5] H. Ashassi-Sorkhabi and S. H. Rafizadeh, Effect of coating time and heat treatment on structures and corrosion characteristics of electroless Ni–P alloy deposits, Surface and Coating Technology vol. 176, 2004, pp. 318–-326.
[6] G. Lu and G. Zangari, Corrosion resistance of ternary Ni-P based alloys in sulfuric acid solutions, Electrochimica Acta, vol. 47, 2002, pp. 2969–2979.
[7] Guo. Z, Keong. K. G and Sha. W, Crystallisation and phase transformation behaviour of electroless nickel phosphorus platings during continuous heating, J. Alloy. Compd., vol. 358, 2003, pp. 112–119.
[8] Erming. M, Shoufu. L and Pengxing. L, A transmission electron microscopy study on the crystallization of amorphous Ni-P electroless deposited coatings, Thin Solid Films, vol. 166, 1988, pp. 273–280.
[9] Keong K G, Sha W and Malinov S, Crystallisation kinetics and phase transformation behaviour of electroless nickel–phosphorus deposits with high phosphorus content, J. Alloy. Compd. vol. 334, 2002, pp. 192–199.
[10] D.J. Levy, Tech. Proc. Am. Electfoplater's SOC.,vol. 50, 1963, pp. 29.
[11] Chassing E., Cherkaoui. M and Srhiri.A, Electrochemical investigation of the autocatalytic deposition of Ni-Cu-P alloys, J. Appl. Electrochem. vol. 23, 1993, pp. 1169–1174.
[12] J. H. Marshall, The nickel metal catalyzed decomposition of aqueous hypophosphite solutions, Electrochem. Soc., vol. 130, 1983, pp. 369–372.
[13] L. M. Abrantes, M.C. Oliveira and E. Vieil, A probe beam deflection study of the hypophosphite oxidation on a nickel electrode, Electrochim. Acta., vol.41, 1996, pp. 1515–1524.
[14] U. Hofmann and K. G. Weill, Dechemma-Monographien, vol.121, 1990, pp. 257.
[15] M. Benabdellah, R. Souane, N. Cheriaa, R. Abidi, B. Hammouti and J. Vicens, Synthesis of calixarene derivatives and their anticorrosive effect on steel in 1M HCl, Pigment Resin Technol., vol. 36, 2007, pp. 373–381.
[16] D.B. Lewis and G.W. Marshall, Investigation into the structure of electrodeposited nickel-phosphorus alloy deposits, Surf. Coat. Technol., vol. 78, 1996, pp. 150–156.
[17] J.P. Bonino, S. Bruet-Hotellaz, C. Bories, P. Pouderoux and A. Rousset., Thermal-stability of electrodeposited NI-P alloys, J. Appl. Electrochem., vol. 27, 1997, pp. 1193–1197.
[18] C.F. Malfatti, J.Z. Ferreira, C.T. Olveira, E.S. Rieder and J.P. Bonino, Electrochemical behavior of Ni-P-SiC composite coatings: Effect of heat treatment and SiC particle incorporation, Materials and Corrosion, vol. 63, 2012, pp. 36–43.
[19] T. Rabizadeh, S. Reza Allahkaram and A. Zarebidaki, An investigation on effects of heat treatment on corrosion properties of Ni–P electroless nano-coatings, Materials and Design, vol. 31, 2010, pp. 3174–3179.
[20] K. Lu, M.L. Sui and R. Lück, Nanostr. Mater., vol. 4, 1994, pp. 465.
[21] K. Lu, Nanostr. Mater., vol. 2, 1993, pp. 643.
[22] H. Lo, W.T. Tsai, J.T. Lee and M.P. Hung, J. Electrochem. Soc., vol. 142, 1995, pp. 91.
[23] I. Paseka and J. Velicka, Hydrogen evolution and hydrogen sorption on amorphous smooth Me-P(x) (Me-Ni, Co and Fe-Ni) electrode, Electrochim. Acta, vol. 42, 1997, pp. 237–242.
[24] M. Lebrini, F. Bentiss, N. Chihib, C. Jama, J.P. Hornez and M. Lagrenée, Polyphosphate derivatives of guanidine and urea copolymer: Inhibiting corrosion effect of armco iron in acid solution and antibacterial activity, Corros. Sci., vol. 50, 2008, pp. 2914–2918.
[25] E. McCafferty, Validation of corrosion rates measured by the Tafel extrapolation method, Corros. Sci., vol. 47, 2005, pp. 3202–3215.
[26] J. L. Carbajal and R. E. White, "Electrochemical production and corrosion testing of amorphous Ni-P," Journal of the Electrochemical Society, vol. 135, 1988, pp. 2952–2957.
[27] R.B. Diegle, N.R. Sorensen, C.R. Clayton, M.A. Helfand, and Y. C. Yu, "XPS Investigation into the passivity of an amorphous Ni-20P alloy," Journal of the Electrochemical Society, vol. 135, 1988, pp. 1085–1092.
[28] S. O. Niass, M. E. Touhami, N. Hajjaji, A. Srhiri, and H. Takenouti, "Inhibiting effect of quaternary phosphine on Ni-P alloys in 1 M HSO," Journal of Applied Electrochemistry, vol. 31, 2001, pp. 85–92.
[29] B. Elsener, M. Crobu, M. A. Scorciapino, and A. Rossi, Electroless deposited Ni-P alloys: corrosion resistance mechanism, Journal of Applied Electrochemistry, vol. 38, 2008, pp. 1053–1060.
[30] R. B. Diegle, N. R. Sorensen, and G. C. Nelson, Dissolution of glassy Ni-P alloys in H//2SO//4 and HCl electrolytes, Journal of the Electrochemical Society, vol. 133, 1986, pp. 1769–1776.
[31] A. Krolikowski, Nature of anodic dissolution of amorphous Ni-P alloys, Materials Science Forum, vol. 185–188, 1995, pp. 799–808.
[32] E. Sikora and D. D. Macdonald, Nature of the passive film on nickel, Electrochimica Acta, vol. 48, 2002, pp. 69–77.
[33] M. G. Fontana and N. D. Greene, Corrosion Engineering, McGraw-Hill, New York, NY, USA, 1967.
[34] Q. Zhao and Y. Liu, Comparisons of corrosion rates of Ni-P based composite coatings in HCl and NaCl solutions, Corrosion Science, vol. 47, 2005, pp. 2807–2815.